Building Engineering 2025, 3(4), 2175.
doi: https://doi.org/10.59400/be2175

Article

Development and characterization of cement paste-coated shape-stabilized phase change materials to achieve net zero energy buildings in desert climates

Khaled Own Mohaisen[1,*], Md. Hasan Zahir[1], Kashif Irshad[1,2], Aasif Helal[3], M. Nasiruzzaman Shaikh[3]

[1] Interdisciplinary Research Center for Sustainable Energy Systems (IRC-SES), King Fahd University of Petroleum & Minerals, Dhahran 31261, Saudi Arabia

[2] Mechanical Engineering Department, King Fahd University of Petroleum & Minerals, Dhahran 31261, Saudi Arabia

[3] Interdisciplinary Research Center for Hydrogen Technologies and Carbon Management (IRC-HTCM), King Fahd University of Petroleum & Minerals, Dhahran 31261, Saudi Arabia

*** Corresponding author:** Khaled Own Mohaisen, Khmohaisen@gmail.com

CITATION

Mohaisen KO, Zahir MH, Irshad K, et al. Development and characterization of cement paste-coated shape-stabilized phase change materials to achieve net zero energy buildings in desert climates. Building Engineering. 2025; 3(4): 2175. https://doi.org/10.59400/be2175

ARTICLE INFO

Received: 29 November 2024
Revised: 28 August 2025
Accepted: 4 September 2025
Available online: 2 October 2025

Abstract: The development of shape-stabilized phase change materials (SS-PCMs) and their use in construction materials has demonstrated significant potential for improving building energy efficiency and reducing the power consumption of buildings, particularly in desert climates. Despite these benefits, the widespread application of PCMs in civil infrastructure is hindered by their high cost, preparation complexity, leakage issues, and low thermal conductivity. This study addresses these challenges by employing a low-cost, lightweight aggregate (LWA) as a carrier combined with polyethylene glycol (PEG) to develop an LWA/PEG composite PCM. The PEG was incorporated into the LWA pores using a vacuum impregnation technique. Analysis via X-ray diffraction (XRD) and Fourier-transform infrared spectroscopy (FTIR) confirmed that the LWA/PEG composite was successfully prepared without any chemical reactions occurring during the process. However, LWA/PEG composite suffers from leakage problems, which limit its use in building applications. Accordingly, a cement paste coating was developed and applied on LWA/PEG to prepare SS-PCM (CLWA) to prevent the leakage of the composite and enhance its thermal conductivity. Moreover, it was noted that the developed CLWA is chemically stable, and it exhibited outstanding thermal stability after 200 cycles of melting and solidification without signs of leakage. These advantageous characteristics indicate that the CLWA developed can be effectively employed to enhance the thermal efficiency of construction materials to achieve net-zero energy in buildings.

Keywords: shape-stabilized PCMs; lightweight aggregates; polyethylene glycol; thermal energy storage concrete; net zero energy buildings

1. Introduction

The cooling of buildings constitutes a significant portion of energy consumption, particularly in hot and arid regions worldwide. To address this issue, various energy conservation strategies have been explored, including the application of insulation [1], materials, and the development of multi-layered glass windows [2], and the use of phase change materials (PCMs) [3–5]. The use of insulation materials decreases energy consumption by reducing the working time of AC units. However, overheating during the summer increases the energy required to maintain thermal comfort in buildings [6].

Phase change materials (PCMs) are widely utilized as thermal energy storage

mediums. They absorb and store energy during the daytime through the melting process and release it at night through solidification [7]. This cyclic process of melting and solidification enables PCMs to capture and release solar energy, contributing to maintaining a stable ambient temperature within buildings [8]. In desert climates, where ambient temperatures can reach up to 50 °C, the energy demand for air conditioning rises significantly. As a result, renewable energy-based strategies for reducing cooling energy consumption are highly appealing. Thermal energy storage offers a promising renewable energy solution due to the abundant sunlight available in such regions. Utilizing phase change materials (PCMs) to capture and store solar energy as latent heat presents a compelling approach for enhancing energy efficiency. Notably, considerable attention has been directed toward identifying suitable PCMs to improve thermal comfort in buildings [9]. Limited data are available on the use of PCMs in buildings under hot weather conditions. It is essential to develop cost-effective and efficient PCMs tailored for use in temperate and hot weather conditions. PCMs are primarily classified based on their phase transition temperatures into four categories: Solid-liquid, liquid-gas, solid-solid, and solid-gas [10]. Among these, solid-liquid PCMs are preferred for energy storage in buildings due to their stability and compatibility with construction materials [11].

A shape-stabilized phase change material (SS-PCM) is a composite system where the PCM is embedded within a porous supporting medium, enhancing its thermal conductivity, chemical stability, and fire resistance while minimizing the risk of leakage [12–14]. The choice of an appropriate PCM combined with a compatible carrier is crucial for applications in hot weather conditions. Studies indicate that desert regions, such as the Arabian Gulf, experience average peak temperatures reaching up to 50 °C during the summer period [15]. Accordingly, A limited number of organic PCMs, such as paraffins, fatty acids, and polyethylene glycol, are suitable for use [16]. Several studies have explored the incorporation of paraffin with various carriers, owing to its exceptional enthalpy and broad operating temperature range [17–22]. However, paraffin experiences significant volume changes (12.5%) [23] during phase transitions, which can compromise the long-term stability of the PCM system. On the other hand, the high cost of fatty acids restricts their commercial use in building applications. The use of PEG is a better candidate for PCM to be utilized in buildings under desert climates. Depending on its molecular weight, PEG has a broad melting temperature range of 3 °C to 69 °C and is chemically stable. Moreover, PEG is cost-effective, non-toxic, and resistant to erosion [24]. In addition, it does not show phase segregation, has a high degree of chemical and physical stability, and a low supercooling value. Furthermore, PEG has a lower vapor pressure and less volumetric change than paraffin [25]. Those advantages make PEG a good PCM candidate for the development of SS-PCM for building applications.

In building applications, the use of lightweight aggregates as a thermal storage carrier is a relatively new topic. To regulate the temperature inside buildings, Memon et al. [26] used a porous lightweight aggregate as a supporting element in conjunction with paraffin. They came to the conclusion that by lowering building interior temperatures, the produced concrete reduced overall energy use [26]. Comparable results have been

noted with PCM made using lightweight particles and lauryl alcohol [27]. To stop leaks, they applied an epoxy coating to their created SS-PCM. Such a technology is not practical for large-scale applications since it needs specific handling, which raises the cost. In order to attain net-zero energy structures, it is necessary to develop a low-cost SS-PCM by combining lightweight aggregates for building applications in desert regions. Scoria is a naturally occurring lightweight aggregate (LWA) with a gray to black hue that finds use in a variety of applications, including filtering media, lightweight concrete, and cost-effective paint filler [28]. In contrast to other pozzolanic materials, scoria is a natural source of pozzolan that can be utilized in mass concretes, according to Alhozaimy et al. [29]. Additionally, various investigations on the application of scoria in lightweight concrete have been conducted [30–32]. Tchamdjou et al. [32] reported that the use of scoria in concrete enhances its properties, such as improving temperature resistance and decreasing shrinkage [30, 31]. Additionally, it has been confirmed that scoria aggregate can be utilized as an ingredient in Portland cement, to make lightweight concrete, and to make blocks [28].

Several methods can be used to penetrate PCM into the carrier. When compared to alternative impregnation techniques, the vacuum impregnation method demonstrated superior PCM absorption [33–35]. According to Ramakrishnan et al. [36], the paraffin/expanded perlite composite made by the impregnation approach has a 30% higher PCM absorption capacity than the same composite made by the direct method. However, they heat the expanded perlite for 24 h at 105 °C, which is inefficient and energy-intensive.

The current research presents the possibilities of using LWA/PEG composite PCM in building applications for desert climates. Using the vacuum impregnation process, LWA has been utilized as a carrier in conjunction with PEG to develop the LWA/PEG composite. Furthermore, the visibility of using a cement paste coating for the developed composite has been addressed to prepare the SS-PCM (CLWA). The results showed the possibility of the developed CLWA to be utilized in construction applications to achieve net-zero energy buildings under desert climates. Furthermore, the developed CLWA has a high melting temperature of 57.7 °C, which significantly exceeds the melting temperature range of most other PCMs (12–31 °C), as summarized in **Table 1**. The elevated melting point of the developed CLWA makes it particularly suitable for applications in hot weather conditions, where lower melting temperature PCMs would be ineffective.

Table 1. Comparison of characteristics of the developed FS-PCM with those reported in the literature.

PCM	Carrier	Melting Temp (°C)	Melting Enthalpy (J/g)	Impregnation method	Coating	Ref
Paraffin	Macro-PCM	18	N/A	N/A	N/A	D'Alessandro et al. [37]
Fatty acids	Diatomite	31.14	154.97	Direct	N/A	Wang et al. [38]
Paraffin	Expanded clay	29.01	102.5	Vacuum	Epoxy/silica	Memon et al. [39]
Butyl stearate	Expanded perlite	12.56	29.26	Impregnation	N/A	Ma and Bai [40]

Table 1. *Cont.*

PCM	Carrier	Melting Temp (°C)	Melting Enthalpy (J/g)	Impregnation method	Coating	Ref
Lauryl alcohol	Lightweight aggregate	22.96	96.65	Vacuum	Epoxy	Cui et al. [41]
Octadecane	Graphite	28	256.5	Vacuum	N/A	Min et al. [42]
Butyl stearate	Lightweight aggregate	20.09	172	Vacuum	N/A	Niall et al. [43]
Capric acid	Expanded Perlite	N/A	12.13	Vacuum	N/A	Kumar et al. [44]
Fatty acid	Pumice + Graphite	31.14	154.97	Vacuum	Epoxy/Cement	Ren et al. [45]
Paraffin	Commercial PCM	28	180	Microencapsulation	N/A	Lecompte et al. [46]
Myristic acid	Attapulgite	22.12	74.97	Direct mix	N/A	Gencel et al. [47]
PEG	Scoria	57.7	35.8	Vacuum	Cement	Current study

2. Materials and techniques

2.1. Materials

The polyethylene glycol (PEG) used was ultrapure (Purity > 99%), with a molecular weight of 6000 g/mol. A quarry in Saudi Arabia's Western Province provided the lightweight aggregate (Scoria), which has a specific gravity of 1.5, a thermal conductivity of 0.27 W/m·K, and an 11% water absorption rate. The aggregate was coated with ordinary Portland cement (OPC), which ASTM C150 classifies as Type I and has a unit weight of 3150 kg/m^3. Fine sand with a specific gravity of 2.56 and a water absorption of 0.60% by weight was utilized as a fine aggregate.

2.2. Fabrication of LWA/PEG composite

The LWA/PEG composite was prepared using the vacuum impregnation method as shown in **Figure 1**. Varying mass fractions of PEG, starting with 20% up to 100% with 20% increments. The impregnation process was conducted using a vacuum pump with a pressure of 0.1 MPa. First, the LWA particles were placed in a conical glass flask, and then the solid PEG was added while applying the vacuum pressure for 10 min. Then a conical vessel was placed in a hot water bath maintained at a temperature of 70 °C for 2 h. The PEG starts melting and impregnating into the pores of LWA due to the applied vacuum and elevated temperature. After 2 h, the PEG ceases to impregnate into the LWA, as can be noticed by the disappearance of air bubbles in the conical glass flask, which indicates that the pores in the LWA are fully filled with PEG. Accordingly, an impregnation time of 2 h, a temperature of 70 °C, and a pressure of 0.1 MPa were selected as optimum conditions. After several trials, it was observed that adding more than 60% PEG led to a greater loss of PEG compared to the weight gained by the LWA pores, without significantly impacting the overall weight gain of the LWA particles. This loss occurred because the pores of the LWA became fully saturated with PEG, preventing further absorption. Therefore, 60% PEG was identified as the optimal quantity for developing the LWA/PEG composite.

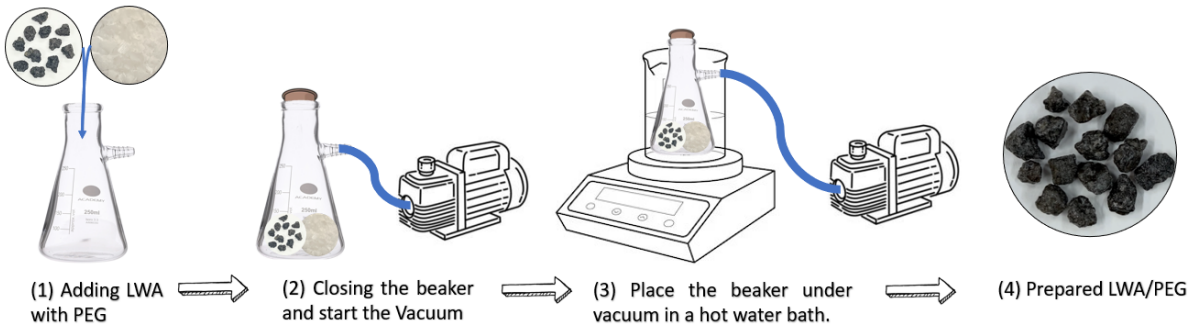

Figure 1. Sketch of the setup used to prepare the LWA/PEG composite.

2.3. Characterization

The mineralogical composition of the materials was determined using a Rigaku X-ray diffractometer (XRD), which used Cu-Kα radiation and operated at 15 mA and 30 kV with a scan rate of 2°/min. A Perkin Elmer (16F PC) spectrophotometer was used to record the Fourier Transform Infrared (FTIR) spectra. The material's morphological analysis was evaluated with a JEOL JSM-6400F FE-SEM running at 10 kV of acceleration voltage. An X-mass detector was also used to record energy-dispersive X-ray spectra (EDS). Differential scanning calorimetry (DSC) measurements were performed by heating 10 mg sealed samples in aluminum pans at a rate of 5 °C/min, under a continuous argon flow of 20 mL/min.

3. Results and discussion

3.1. Particle size distribution of OPC, sand and LWA

The particle size distribution of LWA and fine sand was obtained using sieve analysis, while that of cement was determined using laser diffraction spectroscopy (LDS) using a Microtrac® S3500 laser particle size analyzer, as shown in **Figure 2**. LWA retained on sieve #4 (4.75 mm) was used in the preparation of concrete mixtures. About 84% of LWA was retained on the #4 sieve.

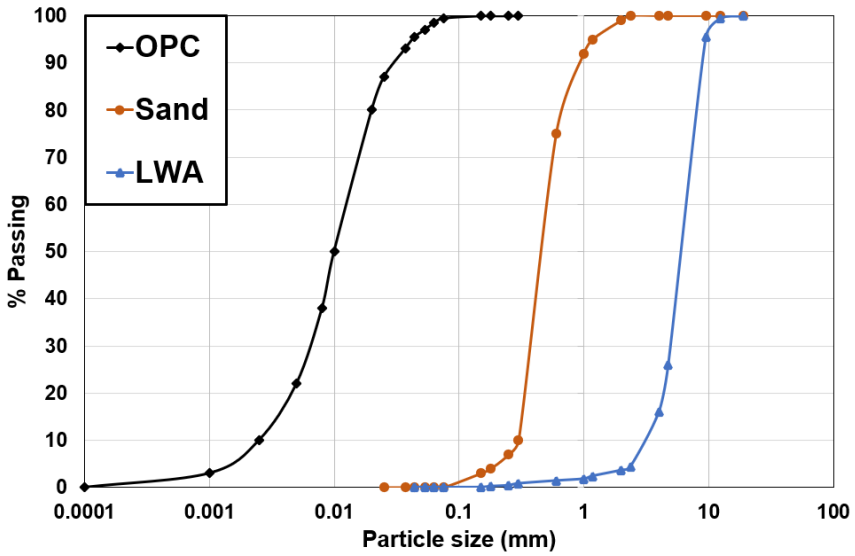

Figure 2. Particle size distribution of OPC, sand, and LWA.

3.2. XRD and FTIR analysis of the LWA, PEG, and the LAW/PEG composites

The XRD peaks for LWA, PEG, and LWA/PEG are shown in **Figure 3**. The peaks located in the range of 20° to 30° 2θ are attributed to the presence of hematite (Fe_2O_3) and anorthite ($Ca(Al_2Si_2O_8)$). The peaks at an angle of 34° 2θ can be ascribed to the formation of aluminum silicate, and those at 60° 2θ indicate the presence of magnetite [48–51]. The LWA/PEG composite exhibited very intense diffraction peaks at 18° and 23° 2θ, which match those obtained for PEG. Moreover, only PEG peaks are present in the LWA/PEG composite, indicating that the developed LWA/PEG formed without any chemical transformation during the injection of PEG into the pores of LWA.

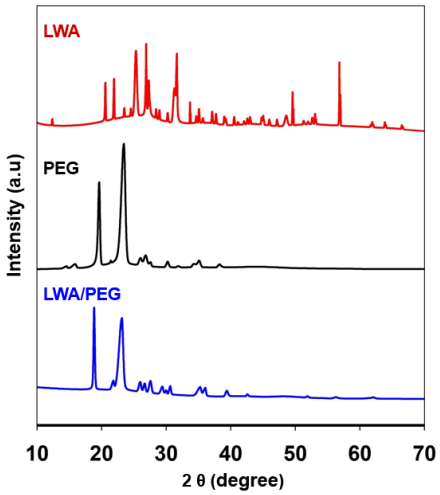

Figure 3. XRD patterns of LWA, PEG, and LWA/PEG composite.

Figure 4 shows the FTIR spectra of LWA, PEG, and LWA/PEG. A broad band in the range of 950 cm^{-1} to 1200 cm^{-1} can be noticed in LWA, which is assigned to the stretching of (Si–O–Si), confirming that SC is mostly composed of silica [49–51]. The spectrum of LWA/PEG closely resembles that of PEG. The lack of significant new peaks in the LWA/PEG spectrum compared to PEG suggests that the formation of the LWA/PEG composite occurs without any accompanying chemical reactions.

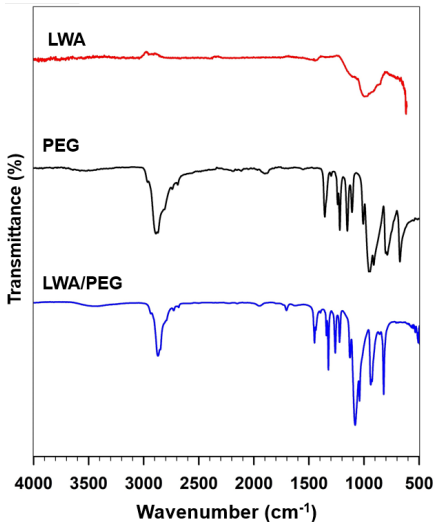

Figure 4. FTIR patterns of LWA, PEG, and LWA/PEG composite.

3.3. Morphology of LWA and LWA/PEG composite

LWA has a highly porous structure, as shown in **Figure 5a**. Varying sizes of Micropores and Mesopores can be noted. This makes the selected LWA have the ability to accommodate a larger quantity of PEG inside these pores to enhance the thermal properties of the developed system. The EDS results in **Figure 5b** show that LWA contains mainly Oxygen (O), Silica (Si), and Iron (Fe), which align with the results obtained from XRD and FTIR. Additionally, the elemental distribution of LWA is shown in **Figure 5c**.

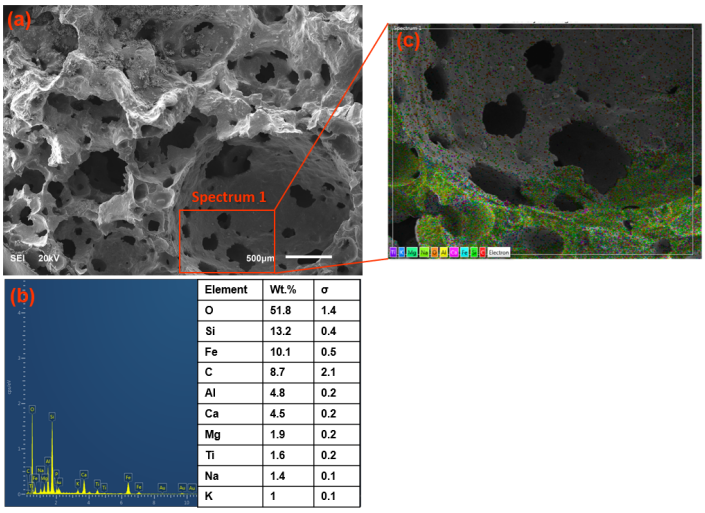

Element	Wt.%	σ
O	51.8	1.4
Si	13.2	0.4
Fe	10.1	0.5
C	8.7	2.1
Al	4.8	0.2
Ca	4.5	0.2
Mg	1.9	0.2
Ti	1.6	0.2
Na	1.4	0.1
K	1	0.1

Figure 5. **(a)** FE-SEM images of LAW and its respective: **(b)** EDS; **(c)** Mapping analysis.

After vacuum impregnation, the pores of the LWA were completely filled with PEG, as illustrated in **Figure 6a**. The elemental analysis of LWA (**Figure 5b**) and the LWA/PEG composite (**Figure 6b**) revealed similar compositions. However, the LWA exhibited higher concentrations of Si, Fe, and Aluminum (Al) compared to the LWA/PEG composite. This reduction is likely due to the presence of PEG occupying the pores of the LWA. Furthermore, the elemental distribution analysis of the LWA/PEG composite presented in **Figure 6c** indicates a uniform distribution of elements, confirming that PEG effectively and comprehensively filled the LWA pores.

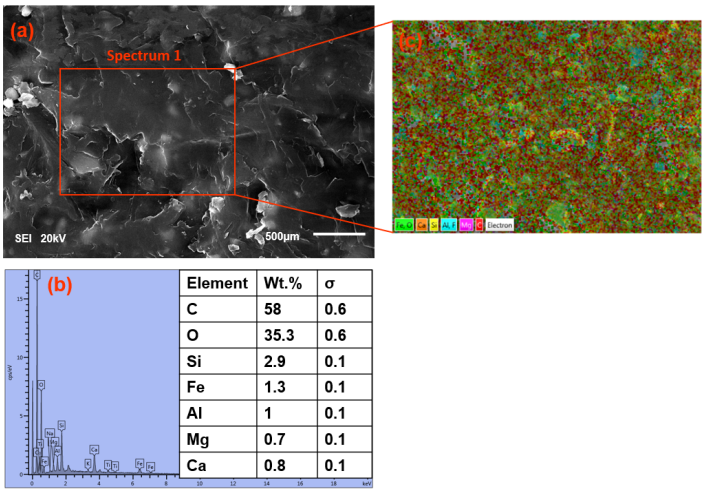

Element	Wt.%	σ
C	58	0.6
O	35.3	0.6
Si	2.9	0.1
Fe	1.3	0.1
Al	1	0.1
Mg	0.7	0.1
Ca	0.8	0.1

Figure 6. **(a)** FE-SEM images of LAW/PEG composite and its respective; **(b)** EDS; **(c)** Mapping analysis.

3.4. Differential scanning calorimetry (DSC)

The DSC curves for the melting and solidification processes of LWA, PEG, and the LWA/PEG composite are presented in **Figure 7**. Enthalpy values were calculated from the areas under the DSC curves corresponding to the melting and solidification cycles. PEG exhibited melting and solidification enthalpies of 192.4 J/g and 191.1 J/g, respectively, aligning with values reported by several researchers [52, 53]. The LWA/PEG composite demonstrated a reduction of approximately 64% and 65% in melting and solidification enthalpies, respectively, compared to pure PEG. This reduction can be attributed to the negligible enthalpy contribution of LWA, because the LWA has no latent heat values (No phase change occurs in the LWA before and after heating). This fact reflects the absence of PCMs in the LWA before the impregnation of PEG. Furthermore, the high melting temperature of the LWA/PEG composite of 58.4 °C makes it an appropriate energy storage system for desert climates.

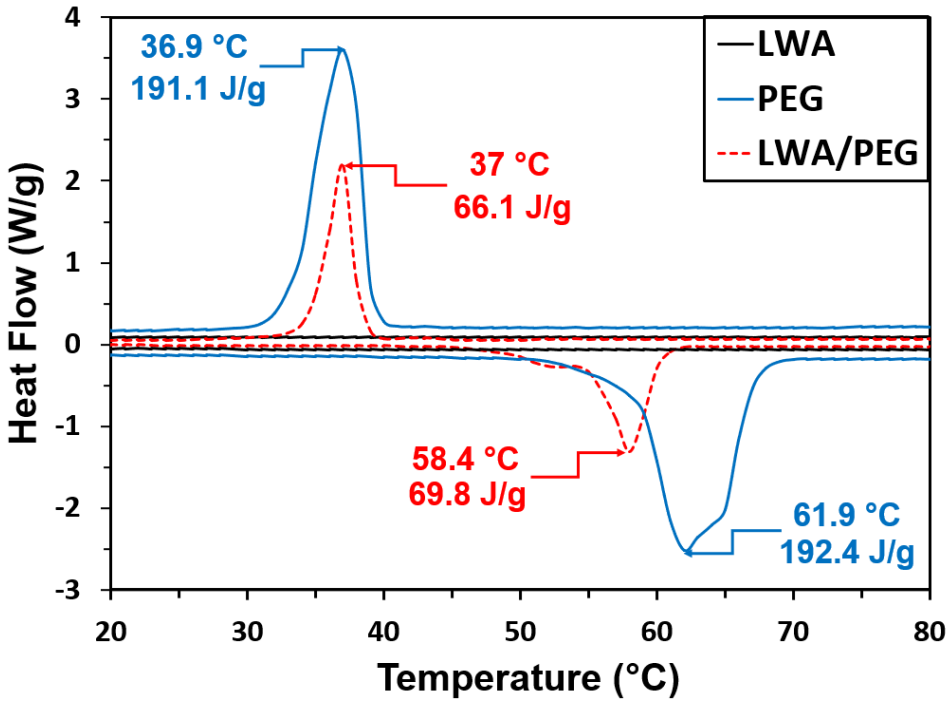

Figure 7. DSC analysis of LWA, PEG, and LWA/PEG.

3.5. Leakage test

Figure 8 illustrates the behavior of PEG and the LWA/PEG composite after exposure to a temperature of 70 °C for 30 min. While PEG completely melted under these conditions, the LWA/PEG composite exhibited minimal leakage, attributed to the presence of PEG on the surface of LWA particles. This observed leakage, as shown in **Figure 8**, highlights a critical limitation, preventing the direct application of leaked PCM into cementitious mixtures due to significant PEG loss [54]. Accordingly, a cement paste coating has been developed to accommodate and prevent the leakage of PEG to obtain the SS-PCM.

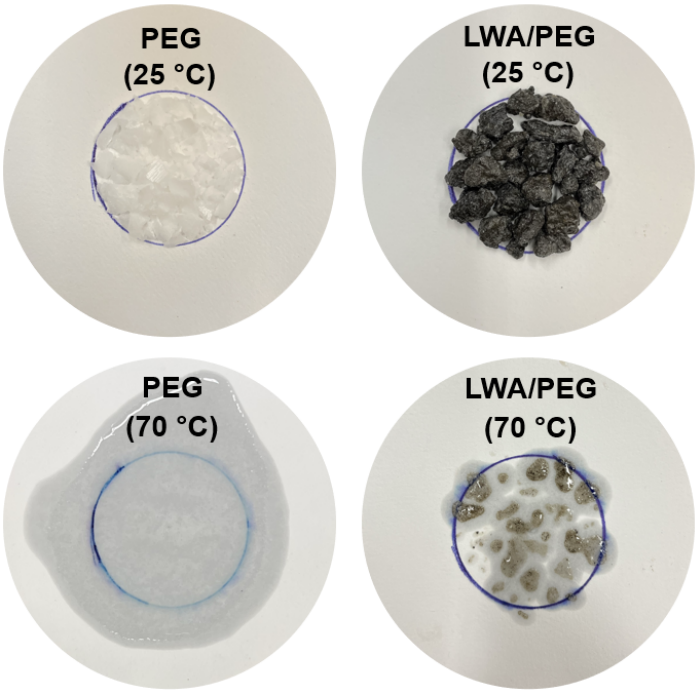

Figure 8. Leakage performance of PEG and LWA/PEG composite.

3.6. Preparation and testing of SS-PCM (CLWA)

3.6.1. Preparation process of CLWA

The cement paste coating was developed by optimizing the LWA/PEG-to-cement ratio through multiple trials. The selected ratio ensured complete coverage of the LWA/PEG particles without leaving excess cement paste. A water-to-cement (w/c) ratio of 0.35 was consistently maintained across all trial mixtures. Initially, the cement and water were mixed for 5 min to achieve a homogeneous paste. Subsequently, the LWA/PEG particles were added to the cement paste and mixed for an additional 5 min until all particles were uniformly coated with a 0.5 mm thick layer of cement paste. The coated LWA (CLWA) was then separated using a sieve and allowed to dry at room temperature for 24 h. After drying, the water absorption and specific gravity of the CLWA were measured in accordance with ASTM C127 [55]. The results showed a water absorption rate of 5.5% and a specific gravity of 1.8, demonstrating the effectiveness of the coating process.

3.6.2. Leakage performance and morphology characteristics of CLWA

The leakage performance of the developed CLWA is presented in **Figure 9**. The CLWA composite exhibited no signs of leakage, even after being subjected to a temperature of 70 °C for 30 min. This result demonstrates that the cement paste effectively encapsulates the PEG within its matrix, successfully preventing any leakage.

The cross-section of CLWA depicted in **Figure 10a** provides insights into the composite inner core structure. As shown in **Figure 10b**, the right portion of the image reveals the formation of calcium silicate hydrate (C–S–H) of the cement coating layer. This observation is further supported by the mapping analysis presented in **Figure 10c**. Additionally, the inner core of the CLWA is filled with PEG, while the cement coating effectively encapsulates the PEG, preventing any leakage from the LWA/PEG

core. This structural configuration highlights the effectiveness of the cement coating in stabilizing the LWA/PEG composite.

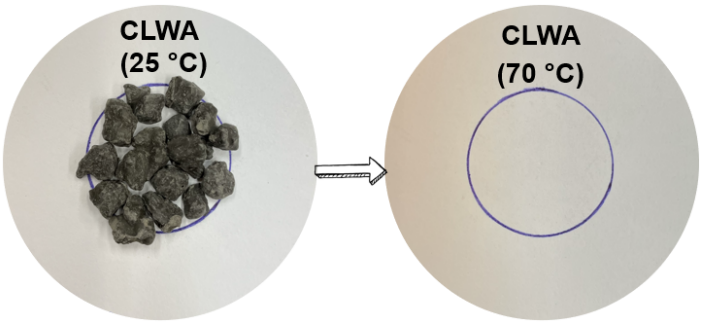

Figure 9. Leakage performance of CLWA.

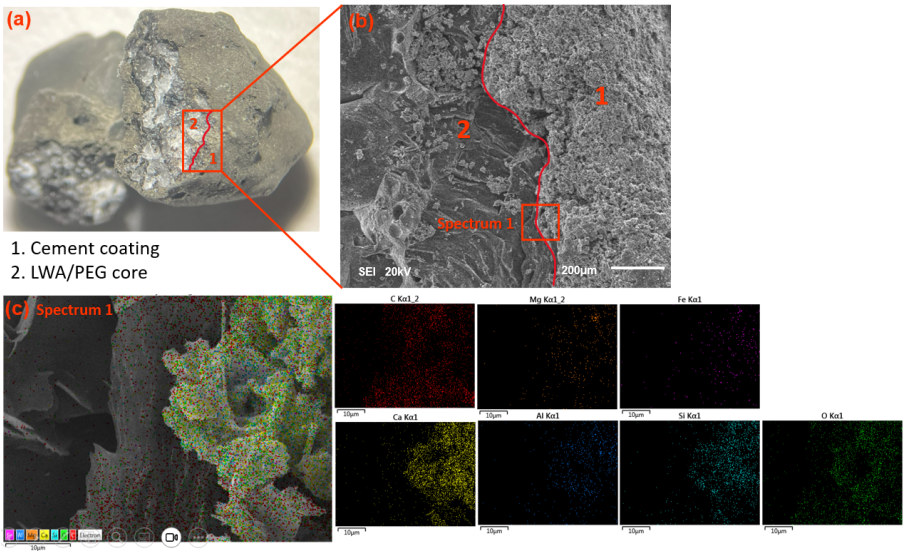

Figure 10. **(a)** Cross-section of CLWA; **(b)** SEM picture of CLWA; **(c)** Mapping analysis of spectrum 1.

3.6.3. Thermal reliability and stability

The thermal reliability of CLWA particles was evaluated by subjecting them to 200 thermal cycles. The DSC results, presented in **Figure 11**, demonstrate that CLWA retains its structural integrity even under rigorous thermal cycling conditions. The material successfully withstood 200 cycles of melting and solidification without significant alterations in its phase change temperatures or enthalpy values. This confirms the excellent thermal stability of the developed CLWA, making it a promising latent heat thermal energy storage material for building applications. Additionally, the melting and solidification temperatures of 56.8 °C and 37.2 °C, respectively, are well-suited for the high ambient temperatures experienced in desert climates during the summer, enhancing the potential of CLWA in reducing energy consumption.

TGA analysis was conducted to assess the thermal stability of the developed CLWA composite. As shown in **Figure 12**, the LWA particles demonstrated no weight loss, indicating their stable thermal behavior. In contrast, the CLWA composite began to lose weight at approximately 350 °C, with the weight loss completing around 400 °C. This loss is attributed to the evaporation of the PEG component from the composite

pores. After this point, the weight of the sample remained constant, indicating that the thermal degradation process had ceased.

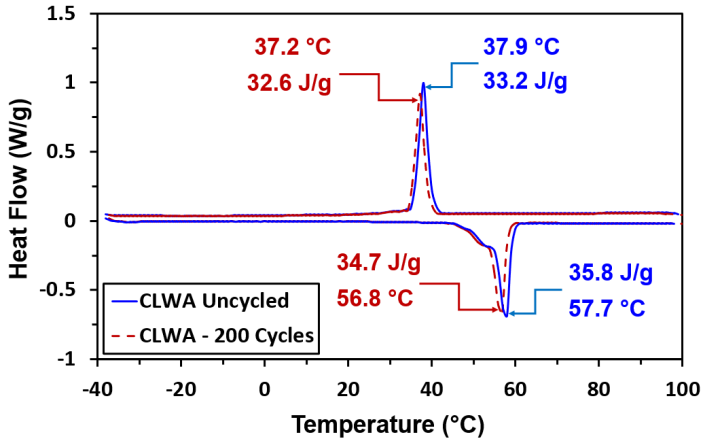

Figure 11. DSC of CLWA composite before and after exposure to 200 thermal cycles.

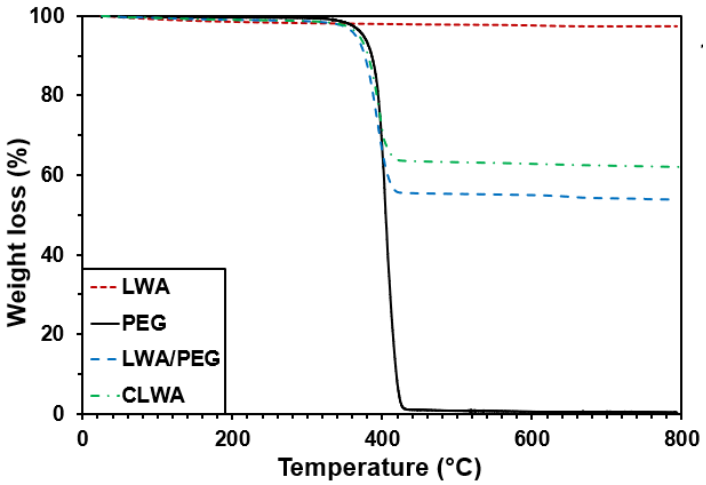

Figure 12. TGA curves of LWA, PEG, LWA/PEG, and CLWA composites.

The weight loss observed in the LWA/PEG composite was 45%, while the weight loss of the CLWA composite was lower. This difference highlights the uniform distribution of PEG within the LWA/PEG composite and supports the conclusion that the preparation process resulted in a homogeneous material. Furthermore, the lower weight loss in CLWA can be attributed to the cement coating applied to the CLWA particles. The cement coating adds mass and enhances the overall stability of the composite, making it more resilient to thermal degradation.

These findings suggest that the developed CLWA composite exhibits robust thermal stability, making it suitable for thermal energy storage applications, particularly in environments such as desert climates. Additionally, the stable thermal behavior of the CLWA composite ensures its long-term reliability in energy storage systems, contributing to efficient thermal regulation in buildings.

Table 2 lists the thermal activity values of PEG and the prepared composites with/without coating.

Table 2. Thermal activity of PEG, LWA/PEG, and CLWA.

Sample	Melting process		Solidification process		Thermal properties					
	T_m (°C)	ΔH_m (J/g)	T_f (°C)	ΔH_f (J/g)	ΔT_s (°C)	E_{eff} (J/g)	R (%)	E (%)	φ (%)	Γ (%)
PEG	61.9	192.4	36.9	191.2	24.9	192.4	-	-	-	100
LWA/PEG	58.4	69.8	37.0	66.1	21.4	148.5	36.3	35.4	97.6	77.2
CLWA	57.7	35.8	37.9	33.2	19.8	76.2	18.6	17.9	96.7	39.6

All the parameters were derived from the following equations:

$$R = \frac{\Delta H_{m,\,com}}{\Delta H_{m,\,PEG}} \times 100\% \tag{1}$$

$$E_{eff} = \frac{\Delta H_{m,\,com}}{X_{PEG}} \tag{2}$$

$$E = \frac{\Delta H_{m,\,com} + \Delta H_{f,\,com}}{\Delta H_{m,\,PEG} + \Delta H_{f,\,PEG}} \times 100\% \tag{3}$$

$$\varphi = \frac{\frac{\Delta H_{m,\,com} + \Delta H_{f,\,com}}{R}}{\Delta H_{m,\,PEG} + \Delta H_{f,\,PEG}} \times 100\% \tag{4}$$

$$\gamma = \frac{\Delta H_{m,\,PEG}}{(x_{PEG} \times \Delta H_{m,\,PEG})} \times 100\% \tag{5}$$

Where: T_m = Melting temperature, ΔH_m = Melting latent heat, T_f = Solidification temperature, ΔH_f = Solidification latent heat, ΔT_f = Supercooling, E_{eff} = Efficient energy per unit mass of PEG as shown in Equation (2) were calculated according to Li et al. [56], R = Impregnation ratio, E = Impregnation efficiency and φ = Energy storage capacity [57] and γ = Heat storage efficiency. In the above equations, com indicates PCM composite (LWA/PEG, CLWA) and X_{PEG} = PEG weight fraction in PCM.

The melting enthalpies of LWA/PEG and CLWA composites decreased by 31% and 64%, respectively, compared to pure PEG, as detailed in **Table 2**. This reduction is attributed to the negligible enthalpies of LWA and the cement paste in CLWA composites. However, the supercooling values of CLWA and LWA/PEG composites were reduced by 14% and 20.5%, respectively, compared to PEG. Notably, the high heat storage efficiency of the CLWA composite makes it a promising candidate for efficient thermal energy storage systems. These characteristics demonstrate the feasibility of employing CLWA in building applications under desert climate conditions. Furthermore, the utilization of CLWA can deliver significant environmental, economic, and sustainable benefits, enhancing and improving the overall quality of buildings subjected to high temperatures in desert environments.

4. Conclusion

In this study, a novel cement-coated LWA/PEG-based PCM was developed to improve the thermal performance of buildings. The following conclusions can be drawn from experimental work.

- A vacuum impregnation technique was effectively utilized to impregnate

polyethylene glycol (PEG) into lightweight aggregate (LWA). The developed LWA/PEG composite exhibited uniform PEG distribution within its pores without any chemical transformations during preparation, as confirmed by XRD and FTIR analyses.

- Cement coating was successfully applied to LWA/PEG composites, addressing the critical issue of PCM leakage. The cement paste encapsulated the PEG, ensuring structural stability and preventing leakage, even under elevated temperatures.
- The CLWA composite exhibited excellent thermal reliability, retaining its structural and thermal properties after 200 cycles of melting and solidification. The negligible changes in phase change temperature and enthalpy demonstrate its suitability for long-term thermal energy storage applications.
- The CLWA composite achieved high heat storage efficiency (96.7%) and demonstrated significant reductions in supercooling compared to pure PEG. These attributes make it a viable material for efficient latent heat thermal energy storage (LHTES) systems.
- The melting and solidification temperatures of CLWA (57.7 °C and 37.9 °C, respectively) align well with the high ambient temperatures experienced in desert climates. This makes it particularly effective in reducing cooling energy consumption in buildings under such conditions.
- The developed CLWA composite is a promising candidate for net-zero energy buildings in desert climates. Its ability to store and release thermal energy efficiently enhances the thermal performance of construction materials, ensuring comfort and sustainability in extreme weather conditions.

Author contributions: Conceptualization, KOM; methodology, KOM; software, KOM; validation, KOM, MHZ; formal analysis, KOM; investigation, KOM; resources, MHZ; data curation, KOM; writing—original draft preparation, KOM; writing—review and editing, KOM, KI, AH and MNS; visualization, KOM; supervision, KOM and MHZ. All authors have read and agreed to the published version of the manuscript.

Funding: This work received no external funding.

Institutional review board statement: Not applicable.

Informed consent statement: Not applicable.

Data availability statement: Not applicable.

Conflict of interest: The authors declare no conflict of interest.

References

1. Aditya L, Mahlia TMI, Rismanchi B, et al. A review on insulation materials for energy conservation in buildings. Renewable and Sustainable Energy Reviews. 2017; 73: 1352–65.
2. Fang Y, Memon S, Peng J, et al. Solar thermal performance of two innovative configurations of air-vacuum layered triple glazed windows. Renewable Energy. 2020; 150: 167–75.
3. Khadiran T, Hussein MZ, Zainal Z, et al. Advanced energy storage materials for building applications and their

thermal performance characterization: A review. Renewable and Sustainable Energy Reviews. 2016; 57: 916–28.
4. Wahid MA, Hosseini SE, Hussen HM, et al. An overview of phase change materials for construction architecture thermal management in hot and dry climate region. Applied Thermal Engineering. 2017; 112: 1240–1259.
5. Keshteli AN, Sheikholeslami M. Nanoparticle enhanced PCM applications for intensification of thermal performance in building: A review. Journal of Molecular Liquids. 2019; 274: 516–33.
6. Sharifi S, Saman W, Alemu A. Identification of overheating in the top floors of energy-efficient multilevel dwellings. Energy and Buildings. 2019; 204.
7. Al Miaari A, Mohaisen KO, Al-Ahmed A, et al. Experimental investigation on thermal management and performance enhancement of photovoltaic panel cooled by a sustainable shape stabilized phase change material. Case Studies in Thermal Engineering. 2025; 67: 105763.
8. Mohaisen KO, Zahir MH, Maslehuddin M, et al. Development of a shape-stabilized phase change material utilizing natural and industrial byproducts for thermal energy storage in buildings. Journal of Energy Storage. 2022; 50: 104205.
9. Javadi FS, Metselaar HSC, Ganesan P. Performance improvement of solar thermal systems integrated with phase change materials (PCM), a review. Solar Energy. 2020; 206: 330–52.
10. Zahir MH, Irshad K, Ibrahim NI, et al. Challenges of the application of PCMs to achieve zero energy buildings under hot weather conditions: A review. Journal of Energy Storage. 2023; 64: 107156.
11. Zhou D, Zhao CY, Tian Y. Review on thermal energy storage with phase change materials (PCMs) in building applications. Applied Energy. 2012; 92: 593–605.
12. Gandhi M, Kumar A, Elangovan R, et al. A review on shape-stabilized phase change materials for latent energy storage in buildings. Sustainability. 2020; 12(20): 18.
13. Zhu N, Li S, Hu P, et al. A review on applications of shape-stabilized phase change materials embedded in building enclosure in recent ten years. Sustainable Cities and Society. 2018; 43: 251–64.
14. Yu K, Liu Y, Yang Y. Review on form-stable inorganic hydrated salt phase change materials: Preparation, characterization and effect on the thermophysical properties. Applied Energy. 2021; 292: 116845.
15. Almazroui M. Summer maximum temperature over the gulf cooperation council states in the twenty-first century: multimodel simulations overview. Arabian Journal of Geosciences. 2020; 13.
16. Bruno F, Belusko M, Liu M, et al. Using solid-liquid phase change materials (PCMs) in thermal energy storage systems. Woodhead Publishing; 2015.
17. Zhang J, Zhang X, Wan Y, et al. Preparation and thermal energy properties of paraffin/halloysite nanotube composite as form-stable phase change material. Solar Energy. 2012; 86(5): 1142–1148.
18. Xu B, Li Z. Paraffin/diatomite composite phase change material incorporated cement-based composite for thermal energy storage. Applied Energy. 2013; 105: 229–237.
19. Li X, Sanjayan JG, Wilson JL. Fabrication and stability of form-stable diatomite/paraffin phase change material composites. Energy and Buildings. 2014; 76: 284–294.
20. Li M, Wu Z, Kao H, et al. Experimental investigation of preparation and thermal performances of paraffin/bentonite composite phase change material. Energy Conversion and Management. 2011; 52: 3275–3281.
21. Lv P, Liu C, Rao Z. Experiment study on the thermal properties of paraffin/kaolin thermal energy storage form-stable phase change materials. Applied Energy. 2016; 182: 475–487.
22. Memon SA, Liao W, Yang S, et al. Development of composite PCMs by incorporation of paraffin into various building materials. Materials. 2015; 8: 499–518.
23. Hasan A, Al-Sallal KA, Alnoman H, et al. Effect of phase change materials (PCMs) integrated into a concrete block on heat gain prevention in a hot climate. Sustainability. 2016; 8(10): 1009.
24. Mohaisen KO, Zahir MH, Al-Dulaijan SU, et al. An innovative lightweight aggregate composite phase change material for thermal energy storage enhancement of concrete under hot weather conditions. Journal of Building Engineering. 2025; 99: 111575.
25. Kou Y, Wang S, Luo J, et al. Thermal analysis and heat capacity study of polyethylene glycol (PEG) phase change materials for thermal energy storage applications. Journal of Chemical Thermodynamics. 2019; 128: 259–274.
26. Memon SA, Cui HZ, Zhang H, et al. Utilization of macro encapsulated phase change materials for the development of thermal energy storage and structural lightweight aggregate concrete. Applied Energy. 2015; 139: 43–55.
27. Cui H, Memon SA, Liu R. Development, mechanical properties and numerical simulation of macro encapsulated thermal energy storage concrete. Energy and Buildings. 2015; 96: 162–714.
28. Moufti MR, Sabtan AA, El-Mahdy OR, et al. Assessment of the industrial utilization of scoria materials in central

Harrat Rahat, Saudi Arabia. Engineering Geology. 2000; 57: 155–162.
29. Alhozaimy A, Fares G, Alawad OA, et al. Heat of hydration of concrete containing powdered scoria rock as a natural pozzolanic material. Construction and Building Materials. 2015; 81: 113–119.
30. Juimo Tchamdjou WH, Cherradi T, Abidi ML, et al. Mechanical properties of lightweight aggregates concrete made with Cameroonian volcanic Scoria: Destructive and non-destructive characterization. Journal of Building Engineering. 2018; 16: 134–145.
31. Bogas JA, Cunha D. Non-structural lightweight concrete with volcanic scoria aggregates for lightweight fill in building's floors. Construction and Building Materials. 2017; 135: 151–163.
32. Tchamdjou WHJ, Grigoletto S, Michel F, et al. An investigation on the use of coarse volcanic scoria as sand in Portland cement mortar. Case Studies in Construction Materials. 2017; 7: 191–206.
33. Song M, Niu F, Mao N, et al. Review on building energy performance improvement using phase change materials. Energy and Buildings. 2018; 158: 776–793.
34. Konuklu Y, Ostry M, Paksoy HO, et al. Review on using microencapsulated phase change materials (PCM) in building applications. Energy and Buildings. 2015; 106: 134–55.
35. Soares N, Costa JJ, Gaspar AR, et al. Review of passive PCM latent heat thermal energy storage systems towards buildings' energy efficiency. Energy and Buildings. 2013; 59: 82–103.
36. Ramakrishnan S, Sanjayan J, Wang X, et al. A novel paraffin/expanded perlite composite phase change material for prevention of PCM leakage in cementitious composites. Applied Energy. 2015; 157: 85–94.
37. D'Alessandro A, Pisello AL, Fabiani C, et al. Multifunctional smart concretes with novel phase change materials: Mechanical and thermo-energy investigation. Applied Energy. 2018; 212: 1448–1461.
38. Wang R, Ren M, Gao X, et al. Preparation and properties of fatty acids based thermal energy storage aggregate concrete. Construction and Building Materials. 2018; 165: 1–10.
39. Memon SA, Cui H, Lo TY, et al. Development of structural-functional integrated concrete with macro-encapsulated PCM for thermal energy storage. Applied Energy. 2015; 150: 245–257.
40. Ma Q, Bai M. Mechanical behavior, energy-storing properties and thermal reliability of phase-changing energy-storing concrete. Construction and Building Materials. 2018; 176: 43–49.
41. Cui H, Memon SA, Liu R. Development, mechanical properties and numerical simulation of macro encapsulated thermal energy storage concrete. Energy and Buildings. 2015; 96: 162–174.
42. Min HW, Kim S, Kim HS. Investigation on thermal and mechanical characteristics of concrete mixed with shape stabilized phase change material for mix design. Construction and Building Materials. 2017; 149: 749–762.
43. Niall D, Kinnane O, West RP, et al. Mechanical and thermal evaluation of different types of PCM–concrete composite panels. Journal of Structural Integrity and Maintenance. 2017; 2: 100–108.
44. Kumar D, Alam M, Sanjayan J, et al. Comparative analysis of form-stable phase change material integrated concrete panels for building envelopes. Case Studies in Construction Materials. 2023; 18: e01737.
45. Ren M, Liu Y, Gao X. Incorporation of phase change material and carbon nanofibers into lightweight aggregate concrete for thermal energy regulation in buildings. Energy. 2020; 197: 117262.
46. Lecompte T, Le Bideau P, Glouannec P, et al. Mechanical and thermo-physical behaviour of concretes and mortars containing phase change material. Energy and Buildings. 2015; 94: 52–60.
47. Gencel O, Ustaoglu A, Benli A, et al. Investigation of physico-mechanical, thermal properties and solar thermoregulation performance of shape-stable attapulgite based composite phase change material in foam concrete. Solar Energy. 2022; 236: 51–62.
48. Kwon JS, Yun ST, Lee JH, et al. Removal of divalent heavy metals (Cd, Cu, Pb, and Zn) and arsenic(III) from aqueous solutions using scoria: Kinetics and equilibria of sorption. Journal of Hazardous Materials. 2010; 174: 307–313.
49. Seyfi S, Azadmehr AR, Gharabaghi M, et al. Usage of Iranian scoria for copper and cadmium removal from aqueous solutions. Journal of Central South University. 2015; 22: 3760–3769.
50. Depci T, Efe T, Tapan M, et al. Chemical characterization of Patnos scoria (Ağri, Turkey) and its usability for production of blended cement. Physicochemical Problems of Mineral Processing. 2012; 48(1): 303–315.
51. Djobo JNY, Tchadjié LN, Tchakoute HK, et al. Synthesis of geopolymer composites from a mixture of volcanic scoria and metakaolin. Journal of Asian Ceramic Societies. 2014; 2: 387–398.
52. Liu Z, Wei H, Tang B, et al. Novel light–driven CF/PEG/SiO2 composite phase change materials with high thermal conductivity. Solar Energy Materials and Solar Cells. 2018; 174: 538–544.
53. Zahir MH, Rahman MM, Irshad K. Shape-Stabilized Phase Change Materials for Solar Energy Storage: MgO and Mg(OH)2 Mixed with Polyethylene Glycol. Nanomaterials. 2019; 9: 1773.

54. Li H, Chen H, Li X, et al. Development of thermal energy storage composites and prevention of PCM leakage. Applied Energy. 2014; 135: 225–233.
55. ASTM. Standard Test Method for Specific Gravity and Absorption of Coarse Aggregate. American Society for Testing and Materials; 2001.
56. Li C, Zhang B, Xie B, et al. Tailored phase change behavior of Na2SO4·10H2O/expanded graphite composite for thermal energy storage. Energy Conversion and Management. 2020; 208: 112586.
57. Qian T, Li J, Min X, et al. Polyethylene glycol/mesoporous calcium silicate shape-stabilized composite phase change material: Preparation, characterization, and adjustable thermal property. Energy. 2015; 82: 333–340.